

# Fatigue Reliability of Offshore Wind Turbines using Gaussian Processes

David Wilkie

*Graduate Student, Dept. of Civil, Environmental, and Geomatic Engineering, University College London, London, UK*

Carmine Galasso

*Associate Professor, Dept. of Civil, Environmental, and Geomatic Engineering, University College London, London, UK*

**ABSTRACT:** The fatigue limit state (FLS) often drives the design of offshore wind turbine (OWT) substructures. Numerical assessment of fatigue damage over the life of a structure is computationally expensive, due to the need for time-history simulation of a large number of environmental conditions. This makes structural reliability for FLS a challenging task as it also requires numerical sampling of random variables to model uncertainty in the estimation of fatigue damage. This paper proposes using Gaussian process regression to build surrogate models for fatigue damage caused by different environmental conditions. A case study demonstrates how the proposed approach reduces the computational effort required to evaluate the FLS. Finally, a structural reliability calculation using the surrogate model highlights the large scatter in fatigue life prediction due to parameter uncertainty.

## 1. INTRODUCTION

Offshore wind power is a growing form of electricity generation. This is particularly true in Europe where most current offshore wind farms (OWFs) utilize offshore wind turbines (OWTs) on monopile foundations to harvest wind energy and generate electricity. The design of these structures is currently specified by prescriptive codes, e.g., IEC 61400-3 (International Electrotechnical Commission 2009). These codes mainly implement the load-resistance factor design (LRFD) approach to achieve a certain safety level in structural components. LRFD is a semi-probabilistic approach, although the implied safety is not always intelligible to design engineers. Specifically, current codes prescribe safety factors and different load combinations to account for structural demand- and capacity-affecting uncertainties, and to ensure ‘safe’ designs over a range of limit states. These factors are currently adapted from the offshore Oil & Gas industry and onshore wind turbines, and have not been specifically calibrated for OWT.

The fatigue limit state (FLS) often drives the design of OWTs (Hubler et al. 2018). Code provisions, e.g. (International Electrotechnical Commission 2009), allow a single combination of wave parameters to be analyzed for each mean wind speed, typically distributed into 2m/s bins. This is a simplification, as environmental parameters vary within bins, and have a complex correlation structure (Hubler et al. 2018). Additionally, 60 minutes worth of simulated OWT behavior is required for each set of environmental conditions, to ensure a stable estimation of damage accumulating over a turbine’s 20-year design life. This makes assessment of an OWTs FLS computationally expensive, and often prevents a full structural reliability assessment. However, the use of reliability analysis would allow better calibration of design-code safety factors and would also allow for potentially more optimized structures (e.g., in terms of costs) through an explicit probability-based design approach. The current, state-of-practice approaches employed to reduce the computational burden for FLS are summarized in the following section.

This paper introduces a fatigue reliability calculation relying on a surrogate modelling technique for efficient fatigue load-case calculation. The proposed approach also allows one to quantify the variability introduced by modelling fatigue parameters as random variables. An illustrative application, combining case-study environmental conditions and an archetype OWT, are introduced in *Section 2*, and these are used in *Section 3* to develop a Gaussian process (GP) surrogate model for FLS analysis. The output from the model is discussed in *Section 4*.

### 1.1. Analysis reduction approaches for FLS

The structural response of an OWT to environmental loading is commonly calculated using computer-based simulators, which require a set of input parameters unique to the OWT and environmental conditions being assessed. The OWT response is predicted through a series of empirical or numerical relationships (Vorpahl et al. 2013). From a high-level perspective, the simulator can be thought of as a ‘black box’ which takes a vector of unique inputs ( $x$ ) and produces an output ( $y$ ) captured by:

$$y = f(x) \quad (1)$$

Time-domain simulation is commonly used to implement Eq. (1) in practice, but, as discussed, it is computationally expensive. Efforts to reduce the computational demand of fatigue analysis for OWTs fall into two categories; either making the analysis more efficient or reducing the total number of simulations required using:

- Load-case reduction;
- Surrogate models;
- Simplified frequency domain models.

Load-case reduction attempts to reduce the computational burden of evaluating a limit state by reducing the number of considered load-cases, by combining those that produce similar damage estimates. This avoids using a statistical model to directly predict response. However, the full structural simulation needs run once (Kuhn 2001).

It therefore does not provide a sufficient saving in terms of computational load to allow for numerical sampling.

Surrogate models replace the simulator in Eq.(1) with an estimator  $\hat{f}(x)$ , which can be fit statistically to outputs from simulator runs at a generic set of inputs (Rasmussen and Williams 2006). Complex linear surrogate model can capture a larger range of behavior than simplified linear models, at the cost of increased complexity and specificity of the model to the training data. One highly flexible type of model consists of a regression built on the use of GPs, which fits an adaptable form to sets of observed data. For instance, (Huchet et al. 2017) found that a GP model was suitable for estimating the FLS of four ‘response topologies’ (analytical surfaces representing different types of possible response: peaked, crested and double peaked) evaluated using the OWT design codes. The GP was fitted to mean wind speed and wind-wave misalignment. Similarly, (Brandt et al. 2017) used a GP model fit to wave height, peak spectral period, mean wind speed, wind turbulence, wind direction and wave direction with small bias. GPs have been fitted to all environmental parameters of a conventional FLS assessment without introducing large model uncertainty. A different approach by (Häfele et al. 2018) consisted of using a GP to summarize fatigue damage against different geometrical parameters to optimize an OWT jacket sub-structure. GP regression has therefore been used in two different contexts: (1) representation of fatigue damage directly against environmental conditions; and (2) to represent lifetime fatigue damage against geometrical properties of the turbine.

The simplified frequency-domain based models are not used in detailed design (Seidel et al. 2016) as they don’t model the complex interaction between control system and mean wind speed.

Surrogate models provide a suitable solution, allowing the use of expensive time-domain simulation with a built-in estimation of uncertainty. However, the different assumptions encoded within a GP have not been compared for OWT on monopiles. Additionally, GPs have not

been used to date to represent the fatigue damage for input into a structural reliability analysis.

## 2. GAUSSIAN PROCESSES APPLIED TO OWT FATIGUE ASSESSEMENT

### 2.1. Fatigue damage calculation

Fatigue damage is cumulative, increasing over a structures operating life as it responds to variable loading. In structural design, fatigue damage is commonly estimated by assuming that the number of load cycles to fatigue failure ( $N$ ) resulting from constant amplitude loading is a function of the applied stress range ( $S$ ) and is represented by an SN-curve (DNV GL 2016). The effect of variable-amplitude loading, caused by stochastic environmental conditions, can be estimated by (1) assuming the ratio of the number of applied cycles to the tolerable number of cycles consumes a fixed proportion of fatigue life; and (2) that the proportion of fatigue life consumed by a load spectrum can be evaluated by summing the fatigue life exhausted by each individual stress cycle (i.e., Miners rule):

$$D_j = \sum_{i=1}^{N_{str}} \frac{n_{ji}}{N_{ji}} = \frac{1}{K_\mu} \sum_{i=1}^{N_{str}} \frac{n_{ji}}{S_{ji}^{-m}} \quad (2)$$

Where  $D_j$  is the total fatigue damage calculated over all  $i$  stress ranges ( $N_{str}$ ) occurring during an analysis (indexed  $j$ );  $m$  is the slope of the SN curve; and  $K_\mu$  is a constant that determines the location of the  $x$ -axis (the number of cycles to failure axis) intersection of the SN curve. To calculate the stress range ( $S_{ji}$ ) and the number of applied cycles ( $n_{ji}$ ) in Eq. (2), a structural simulation is run at a specific combinations of environmental parameters and stresses at the seabed are extracted. The fatigue damage ( $D_{j,life}$ ) is then scaled linearly from the analysis length ( $T_{analysis}$ ) to the life of the structure ( $T_{life}$ ):

$$D_{j,life} = \frac{T_{life}}{T_{analysis}} \cdot D_j \quad (3)$$

### 2.2. Fatigue limit state equation

A limit state function,  $G$ , defines whether a structure satisfies the performance target defined by the limit state being assessed. In the FLS, this is whether the fatigue damage accumulated during the OWT life is large enough to threaten the structure. In Eq. (3), fatigue damage is calculated for a single environmental state which is assumed to persist over the entire life of the OWT. However, in practice, a large variety of environmental conditions occur. The damage predicted by Eq. (3) ( $D_{j,life}$ ) is weighted by the probability of occurrence of the corresponding environmental conditions ( $P_j$ ):

$$G(x_\delta, x_{SN}) = x_\delta - x_{SN} \left[ \sum_{j=1}^{N_{smp}} D_{j,life} \cdot P_j \right] \quad (4)$$

If  $G(x_\delta, x_{SN})$  is below zero, the OWT is assumed to fail during its life, as the accumulated fatigue damage is larger than the fatigue damage capacity. Uncertainty in the fatigue capacity ( $x_\delta$ ) and SN curve ( $x_{SN}$ ) parameters are captured by modelling them as random variables. The  $N_{smp}$  term is the number of samples.

The probability of failure can then be evaluated by plain Monte Carlo sampling the uncertain variables and averaging over the number of limit state samples ( $N_{LSsmp}$ ):

$$P_f = \frac{1}{N_{LSsmp}} \sum_{i=1}^{N_{LSsmp}} I(G_i(x_\delta, x_{SN})) \quad (5)$$

In Eq. (5),  $I(\cdot)$  is an indicator function which has a value of one if the limit state sample  $G_i(x_\delta, x_{SN})$  is negative (the structure fails). The probability of failure  $P_f$  is then equivalent to an expectation over the indicator function .

### 2.3. Surrogate model definition

The damage term in Eq. (4) can be evaluated using a surrogate model instead of the computationally expensive structural simulation. GP regression is used here, assuming that the observed data is drawn from an underlying stochastic process.

Estimates for new data can then be generated by conditioning the process on the observations. When applied to a practical regression problem, the GP reduces from an infinite dimensional process to a finite dimensional multivariate Gaussian distribution, due to the marginalization feature of Gaussian distributions (e.g., Rasmussen and Williams 2006).

Predictions of unknown test values ( $y^*$ ) are generated by conditioning the GP on training observations, comprising pairs of output observations ( $\mathbf{y}$ ) and input environmental conditions ( $\mathbf{x}$ ). This results in a multivariate conditional Gaussian distribution defined by a mean ( $\mu_{x^*}$ ) and a covariance ( $\Sigma_{x^*}$ ) function:

$$\begin{aligned} \Pr(y^* | \mathbf{x}^*, \mathbf{x}, \mathbf{y}) &\sim N(\mu_{x^*}, \Sigma_{x^*}) \\ \mu_{x^*} &= \mathbf{k}_{x^*,x} (\mathbf{k}_{x,x} + \sigma_n^2 \mathbf{I})^{-1} \mathbf{y} \\ \Sigma_{x^*} &= \mathbf{k}_{x^*,x^*} - \mathbf{k}_{x^*,x} (\mathbf{k}_{x,x} + \sigma_n^2 \mathbf{I})^{-1} \mathbf{k}_{x,x^*} \end{aligned} \quad (6)$$

In Eq. (6),  $\sigma_n^2$  models the noise about the observed values and  $\mathbf{I}$  is an identity matrix that assigns the it to diagonal terms of the  $\mathbf{k}_{x,x}$  matrix.

The training observation values  $\mathbf{y}$  at input locations  $\mathbf{x}$  enter directly into the conditional mean prediction equation as a linear combination of training sample observations ( $\mathbf{y}$ ).

The value of each entry in the covariance matrix can be calculated using a kernel, i.e., a function modelling the relationship between the input data. The form of the kernel function is variable and encodes assumptions about the relationship of the response at different location in the regression. One common choice is the squared-exponential kernel function (Rasmussen and Williams 2006) which is defined based on the magnitude of the distance between two input vectors, and results in a smooth regression surface.

In this paper the GP, given in Eq. (6), is conditioned on observations of fatigue damage predicted using a computationally expensive time-domain dynamic analysis. In this context  $\mathbf{x}$  is a set of environmental conditions and  $\mathbf{y}$  is the vector corresponding to fatigue damage values ( $D_{j,life}$ ) predicted using the analysis model. Prediction of

lifetime fatigue damage ( $y^*$ ) can be made for sets of input environmental conditions ( $\mathbf{x}^*$ ) that have not been explicitly evaluated.

Table 1: Probability distributions used to model environmental conditions at the FINO 3 site.

Variable	Distribution	Dependency	Limits
$V_w$	Weibull	N/A	[4;24]
$T_i$	Weibull; Gamma	$V_w$	[0.01;0.18]
$H_s$	Gumbel; Weibull	$V_w$	[0.01;7]
$T_p$	Bimodal Gumbel	$H_s$	[1;15]
$\theta_{wind}$	Non-parametric KDE	$V_w$	[0;180]
$\theta_{wave}$	Non-parametric KDE	$H_s; T_p$	

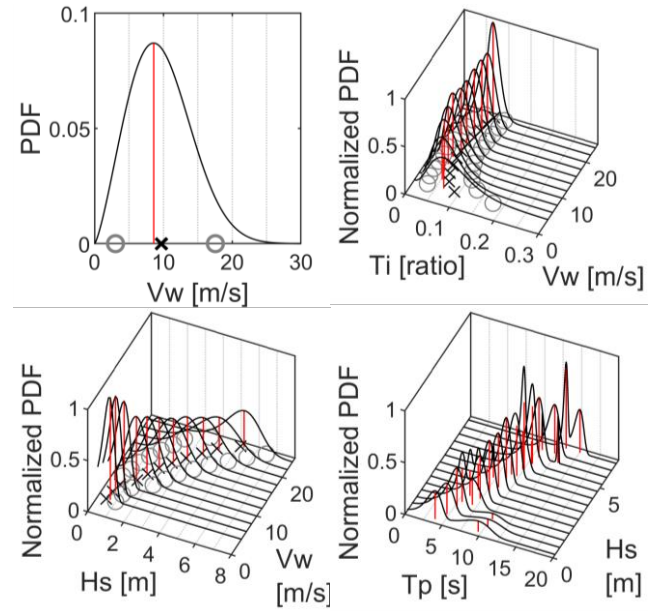


Figure 1. Environmental conditions measured at the FINO 3 site. The mean of each distribution is identified by an 'x', the 0.05 and 0.95 quantiles by a circle, and the mode by a red line.

### 3. ILLUSTRATIVE APPLICATION

#### 3.1. Case-study site

This study uses environmental data measured at the FINO3 met-mast, located in the German sector of the North Sea. Measured site environmental data was post-processed into joint-environmental distributions by (Hübler et al. 2017). The environmental conditions utilized in this work were: the mean wind speed ( $V_w$ ), turbulence

intensity ( $T_i$ ), peak spectral period ( $T_p$ ), significant wave height ( $H_s$ ), wind inflow angle ( $\theta_{wind}$ ) and wave inflow angle ( $\theta_{wave}$ ). The full set of dependencies are summarized on Table 1, and the non-angle variables are plotted on Figure 1, to show the dependencies and variation of conditions within 2m/s mean wind speed bins. In the subsequent analysis the wind and wave inflow angle were combined into a single variable, misalignment ( $\theta_{mis}$ ), reducing the number of environmental variables to five.

### 3.2. OWT numerical model

The 3-bladed NREL 5MW OWT on monopile sub-structure (Jonkman et al. 2009) is used as the reference structure in this study. A list of full dimensions and material properties are provided by (Jonkman et al. 2009). The turbine is operational between mean wind speeds 3m/s to 25m/s and the rated rotor speed is 12.1rpm. The structural response of the OWT to different environmental conditions is calculated in the time-domain using the aero-hydro-elastic wind turbine simulation package FAST (Jonkman and Jonkman 2015). Within the structural model the OWT foundations were modelled using the apparent fixity method (Zaaijer 2006).

Analysis time series were generated in 10-minute-long sets. The stress time history is repeated 36 times, generating a 6-hour long time series. This mitigates against the observed increases in predicted fatigue damage with increased analysis length which is due to the effect of unclosed cycles in the rainflow counting algorithm (Hübler et al. 2017), as ratio of unclosed to closed cycles is reduced by duplicating the stress time history. The rainflow counting algorithm is then used to extract the magnitude and number of different stress ranges occurring within the 6-hour stress time history, allowing fatigue damage to be estimated using Eq. (2).

Fatigue damage is calculated for a single weld located at the mudline. The weld is a transverse butt weld with no weld toe grinding (DNV class D (DNV GL 2016)) and it is assumed to be protected from corrosion by cathodic protection. The DNV

SN curves are bi-linear in the log scale. To simplify the limit state calculation, only the initial part of the SN curve is used, making the curve linear. Fatigue damage is estimated using this method at 12 locations equally distributed around the piles mudline cross-section, with the largest value being extracted for use in the fatigue life calculation.

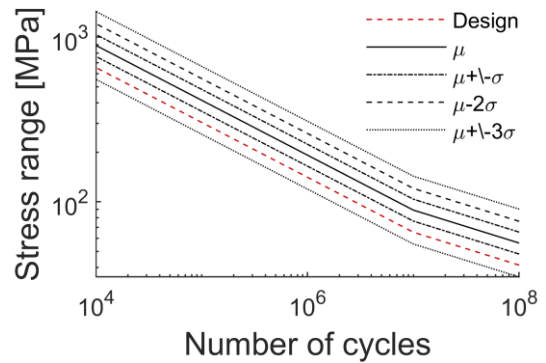


Figure 2. DNV SN curve, showing experimental mean, standard deviations and design curve.

### 3.3. Uncertainty – SN curves

The linear damage accumulation approach contains uncertainty in both the SN curve and the tolerable damage at failure (DNV GL 2016). In current design, the SN curve is fit to data from experimental tests and a linear relationship is fitted to the data. However, these tests exhibit large variability and in fatigue design, the 10<sup>th</sup> percentile of experimental typically data is used as a “design curve”. This introduces a large quantity of conservatism into designs according to this method, as indicated on Figure 2. In Eq. (4), the fatigue curve parameters were included as random variables, to capture the uncertainty in the experimental data (DNV GL 2015). The tolerable damage ( $x_\delta$ ) term is modelled as a lognormal random variable with normal mean equal to one and normal standard deviation 0.3; the SN uncertainty ( $x_{SN}$ ) is modeled as a lognormal with mean -0.91 and standard deviation 0.46; the effect of such assumption on the SN curve is shown in Figure 2.

### 3.4. Training/Testing data

Training sets were used to fit the GP models and a validation set was used to compare the quality of

different surrogate models. The training and validation set were each generated using a sample of 1,000 analyses (each with 6 seeds) drawn randomly from the input environmental distributions. These samples were constructed sequentially by taking 1,000 uniformly distributed random numbers for each variable and using the inverse cumulative distribution functions (iCDF).

### 3.5. Statistical model fitting

The GP model is fitted to the training data by using maximum likelihood estimation. Different assumptions concerning the form of the GP were tested, as described by (Rasmussen and Williams 2006), including:

- Kernel function: squared exponential (SE), Matern 3/2, Matern 5/2 and rational quadratic.
- Underlying function on which the GP is fit: none and linear function.
- Inputs: not standardized and standardized (i.e. inputs converted to approximate standard normally distributed form).

An estimation of total lifetime fatigue damage can then be generated by integrating damage at individual environmental conditions ( $D_{j,life}$ ) across the site joint probability distribution (the term inside the square brackets in Eq. (4)). The damage integration is solved using Monte Carlo sampling with 1,000,000 random samples drawn from the GP and joint PDF between the upper and lower bounds on Table 1.

Each combination of kernels was tested, with the accuracy of the resulting GP evaluated using three metrics: (1) Bias;  $Bias = \mathbb{E}[\hat{y}_i - y_i]$ , indicating whether the predictor consistently under- or over- predicts results. (2) Mean squared error;  $MSE = \frac{1}{n-p} \sum (\hat{y}_i - y_i)^2$ , measuring the expected error. (3) Coverage of the 50% and 95% confidence intervals, e.g. for a well-calibrated model around ~50% of the validation observations should fall within the 50% confidence intervals. The metrics rely on: estimate at the  $i^{th} \in [1, n]$  validation point ( $\hat{y}_i$ ); the observed value at each validation point ( $y_i$ ) predicted using FAST; and

the number of dimensions of the predictor ( $p$ ), which is 5.

## 4. RESULTS

### 4.1. Goodness of fit / Kernels

All combinations of kernel function, basis function, and standardization listed in Section 3.5 are tested, with a summary of the key results in Table 2. Validation from the SE and Matern 5/2 kernels, shown on Figure 3, confirm the slightly reduced bias and scatter observed with the Matern kernel; however, the coverage metrics were slightly worse. The Matern 5/2 was best with both sample sets and is used in remainder of this paper. These findings agree with (Häfele et al. 2018) who found this kernel represented joint fatigue loads for an OWT on a jacket substructure well.

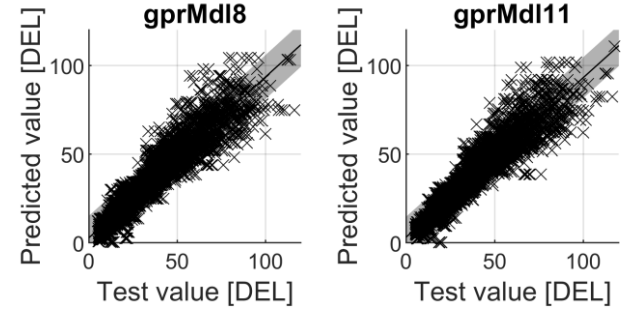


Figure 3. Validation plots for two GP models in terms of design equivalent load (DEL) (Seidel et al. 2016).

### 4.2. Number of samples

The computational burden required to run the 6,000 structural simulations is large. Additionally, the standard GP algorithm retains all training points, making models with large training samples slower. Any reduction in the required number of samples has a double benefit. However, in advance, it is not clear whether reducing the number of samples or seeds will have a greater impact on the accuracy of the surrogate model. The number of seeds will change the number of analyses at a specific set of input conditions and may improve the coverage metrics (as noise at each input point will be defined better). Whereas changing the number of samples will affect the sampling quality over the input conditions, which should effect the mean square error.

Different numbers of random samples and seeds were tested by drawing sets of 1,000 bootstrapped samples from the full set of analysis results (1,000 · 6); the consequent scatter in goodness of fit metrics were assessed for these reduced analysis sets. The results, presented on Figure 4, suggest that both the number of samples and seeds can be reduced without a large impact on the mean squared error and the coverage. In the remainder of this paper an analysis set is used consisting of two seeds (because of coverage and MSE metrics) and 300 samples (because of MSE).

### 4.3. Reliability calculation

Reliability assessment was implemented using Eq. (5), evaluated with 2,000,000 limit state samples. Modelling the SN random variable resulted in predictions of lifetime fatigue damage with scatter,

shown on Figure 5, with CoV 0.063. The limit state values, also include randomness in tolerable damage, plotted on Figure 6, also showing a best fit GEV distribution. The probability of failure over a 20-year design life is  $8.63e-4$ . Scatter in the limit state is caused by the uncertainty in the SN curve and tolerable damage, and the best fit GEV has a CoV of 0.394, indicating high uncertainty introduced by modelling tolerable damage as a random variable. Within the limit state equation, the two random variables act against each other: the SN curve randomness increases capacity (as the design curve is conservative), whereas modelling tolerable damage as random reduces capacity (because the median is below one).

This results in ~22% of limit state samples falling below the limit state predicted using the design SN curve and damage tolerance of 1.

Table 2: Kernel parameters and fitting metrics for a subset of the GP used to represent fatigue damage.

Gaussian process type	1000*6		300*2						
	SE kernel [gprMdl1]	Matern 5/2 kernel [gprMdl1]	SE kernel [gprMdl1]	Matern 3/2 kernel [gprMdl1]	Matern 5/2 kernel [gprMdl1]	Rational quadratic kernel [gprMdl12]	Standardised ; matern 5/2 kernel [gprMdl14]	Basis function matern 5/2 kernel [gprMdl1]	Standardised; basis function matern 5/2 kernel [gprMdl16]
<i>Sigma:</i>	4.128	3.412	4.297	3.429	3.830	3.290	3.830	3.439	3.191
<i>LengthScale1 (Vw)</i>	2.428	4.745	29.949	66.325	39.538	[N/A]	9.659	30.533	0.760
<i>LengthScale2 (Ti)</i>	0.513	0.848	0.704	1.095	0.809		30.391	0.490	0.002
<i>LengthScale3 (Hs)</i>	1.823	2.930	2.115	2.321	1.963		1.928	0.933	0.542
<i>LengthScale4 (Tp)</i>	0.946	1.705	1.291	2.596	1.849		1.202	1.118	0.276
<i>LengthScale5 (θ<sub>Mis</sub>)</i>	55.194	75.197	52.879	98.203	78.049		1.740	44.711	117.778
<i>SigmaF</i>	32.382	35.309	34.303	31.323	29.726	58.929	29.726	15.562	14.693
<i>LogLikelihood</i>	-6312	-6036	-1891	-1855	-1871	-1857	-1871	-1853	-2113
<i>Bias</i>	-0.455	0.059	-0.354	-0.246	-0.246	-0.192	-0.246	-0.153	0.644
<i>MSE</i>	45.322	29.513	41.270	37.012	36.515	40.064	36.515	39.471	204.410
<i>Coverage: 95%</i>	0.935	0.931	0.925	0.927	0.927	1.	0.927	0.925	0.949
<i>50%</i>	0.669	0.682	0.627	0.642	0.639	0.649	0.639	0.639	0.643

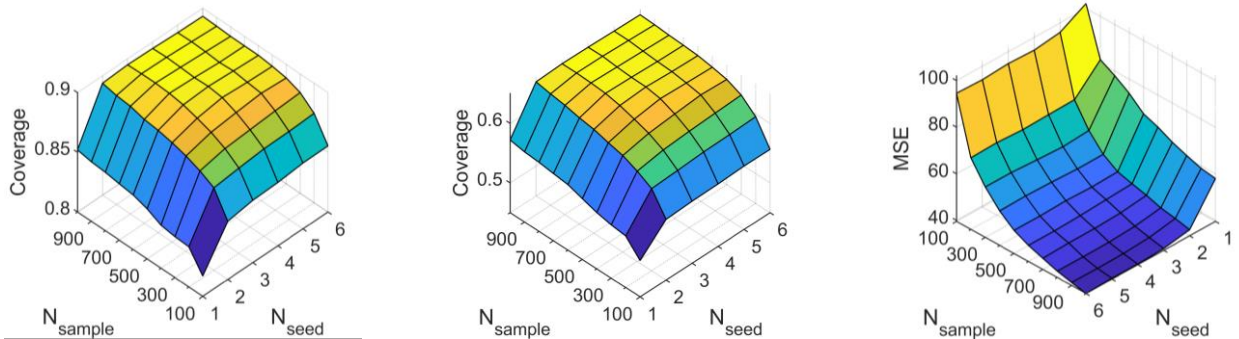


Figure 4. Impact of number of samples and number of seeds on GP accuracy, showing: 90% coverage (left), 50% coverage (middle) and MSE (right).

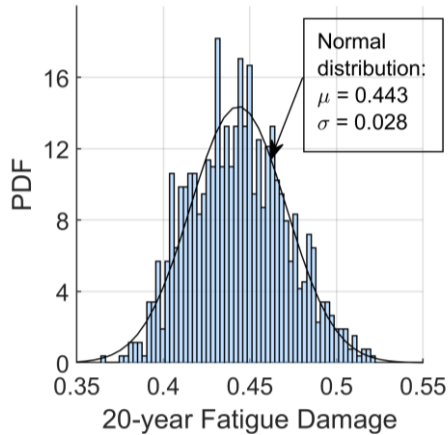


Figure 5. Histogram of 20-year fatigue damage values when SN uncertainty is modelled.

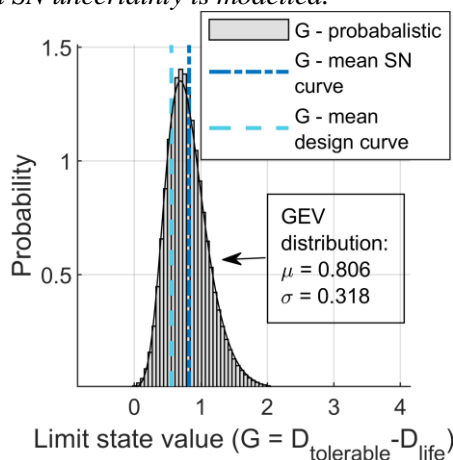


Figure 6. Histogram of limit state values when fatigue material parameters were modelled as random variables.

## 5. CONCLUSION

GP regression is a suitable method for reducing the computational burden of evaluating the FLS for OWT structures. It results in a statistical model that is interpretable and, additionally, also allows efficient reliability assessment. In this paper, the SN uncertainty and tolerable fatigue damage were modelled as random variables, indicating the large scatter these parameters introduce into evaluation of the fatigue limit state.

## 6. ACKNOWLEDGEMENTS

This work was supported by the UK Engineering and Physical Sciences Research Council (EPSRC), DTP grant EP/M507970/1 and the UCL Legion High Performance Computing Facility (Legion@UCL).

## 7. REFERENCES

- Brandt, S. et al (2017). "Meta-models for fatigue damage estimation of offshore wind turbines substructures." *Procedia Engineering*, 199.
- DNV GL. (2015). *Probabilistic methods for planning of inspection for fatigue cracks in offshore structures*.
- DNV GL. (2016). *Fatigue design of offshore steel structures*.
- Häfele, J. et al (2018). "A Systematic Approach to Offshore Wind Turbine Jacket Pre-Design and Optimization: Geometry, Cost, and Surrogate Structural Code Check Models." *Wind Energy Science*, (May).
- Hubler, C., Gebhardt, C. G., and Rolfes, R. (2018). "Methodologies for fatigue assessment of offshore wind turbines considering scattering environmental conditions and the uncertainty due to finite sampling." *Wind Energy*, (May).
- Hübler, C., Gebhardt, C. G., and Rolfes, R. (2017). "Development of a comprehensive data basis of scattering environmental conditions and simulation constraints for offshore wind turbines." *Wind Energy Science*, 2(2015).
- Huchet, Q. et al (2017). "The help of metamodels for the wind turbine certification." (August).
- International Electrotechnical Commission. (2009). *IEC 61400-3. Wind turbines - Part 3: design requirements for offshore wind turbines*.
- Jonkman, B., and Jonkman, J. (2015). *FAST Readme v8.12.00a-bjj*. Denver.
- Jonkman, J. et al (2009). *Definition of a 5-MW reference wind turbine for offshore system development*.
- Kuhn, M. (2001). "Dynamics and design optimization of offshore wind conversion systems." Delft University of Technology.
- Rasmussen, C., and Williams, C. (2006). *Gaussian processes for machine learning*. MIT Press, Cambridge.
- Seidel, M., Voormeeren, S., and van der Steen, J.-B. (2016). "State-of-the-art design processes for offshore wind turbine support structures." *Stahlbau*, 85(9).
- Vorpahl, F. et al (2013). "Offshore wind turbine environment, loads, simulation, and design." *Wiley Interdisciplinary Reviews: Energy and Environment*, 2(5).
- Zaaijer, M. B. (2006). "Foundation modelling to assess dynamic behaviour of offshore wind turbines." *Applied Ocean Research*, 28(1).